



Optoelectronic Properties of ZnO Thin Films Grown by Sol-Gel Technique

Surajit Mandal, Physics, Burdwan Raj College, India

Article Record: Received Sept. 24 2017, Revised paper received Nov. 28 2017, Final Acceptance Dec. 3 2017
Available Online December 7 2017

Abstract

The structural as well as optical properties of nanocrystalline ZnO films, with hexagonal shaped particles of size 30-35 nm grown on glass (100) substrates by sol-gel technique, are investigated. X-ray diffraction patterns of annealed films reveal the formation of wurtzite structure. The mechanism of ultraviolet (UV) and green emission from ZnO thin films, post-annealed at various temperatures, is investigated using photoluminescence spectra. The oxygen content in annealed ZnO films plays an important role to suppress the green band emission. Luminescence is an important material property because it can provide information on defects and relaxation pathways of excited states.

Keywords: *ZnO Nanocrystal, Thin Film, Optical Property, Sol-Gel Technique*

1. Introduction

Zinc oxide, an II–VI semiconductor with a wide direct band gap of 3.3 eV and large exciton binding energy ~60 meV at room temperature (Liang et al., 1968), is especially attractive for optoelectronic, nonlinear optics and electro optics (Kityk et al., 2002) applications. ZnO based films have been used for several applications in transparent conductive layer, solar cell windows, and bulk acoustic wave devices (Yang et al., 1998). The optical properties of ZnO make it one of the most promising materials for photonic devices in the ultraviolet range. Moreover, the binding energy of the exciton of ZnO (60 meV) is larger than its competitor GaN (25 meV) at room temperature making it attractive (Lu et al., 2000) for exciton-related device applications. Several techniques have been used to fabricate ZnO films, including chemical vapor deposition (Bethke et al., 1988), molecular beam epitaxy (Ko et al., 2000), sputtering (Jeong et al., 2003), pulsed laser deposition (Shan et al., 2004) and sol-gel technique (Natsume et al., 2002). Of these techniques, sol-gel route is very attractive with excellent control over composition and relatively easier fabrication of a large area film at a low cost. Stoichiometric zinc oxide is an insulator with the wurtzite structure. The structure contains large voids, which can easily accommodate interstitial atoms. Consequently, it is virtually impossible to prepare pure crystals; also, they tend to lose oxygen when heated to a very high temperature (Azaroff, 1960). For these reasons, ZnO exhibits *n*-type semiconducting properties with inherent defects, such as the lack of O and the excess of Zn. In this regard, the study of the photoluminescence (PL) characteristics of ZnO is interesting because it can provide valuable information on the quality and purity of the materials. Moreover, the low temperature PL study also shows the interactions of the nano-confined trapping states and lattice sub-systems (Williams et al., 2006). It is well agreed that the ultraviolet emission of ZnO is attributed to the exciton emission originating from the recombination of free excitations through an exciton-exciton collision process (Fonoberov et al., 2006), while the mechanism of the blue-green emission relates to the oxygen vacancy or Zn interstitials. It has been reported that the singly ionized oxygen vacancy is responsible for the green emission, since the

emission results from the recombination of a photo generated hole with the singly charged oxygen vacancy (Vanheusden et al., 1996). These oxygen vacancies have comparatively low formation enthalpy (Zhang et al., 2001) and are dependent on the oxygen deficiency in the film.

2. Objectives of the Study

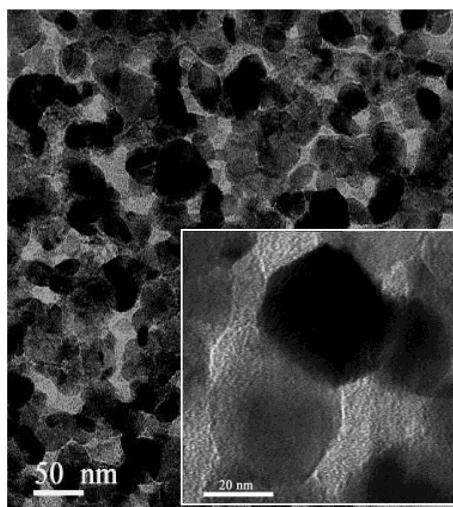
In this paper, we report the growth and optical characteristics of nanocrystalline ZnO films on glass substrates deposited by sol-gel technique. The microstructure and morphology of ZnO films were characterized by X-ray diffraction. The optical properties of grown ZnO thin films annealed at different temperatures were investigated using photoluminescence and UV-spectroscopy. The effect of post-deposition annealing treatment on the mechanism of UV and green emissions of nanocrystalline ZnO thin films are studied.

3. Experimental

Zinc acetate dihydrate ($\text{Zn}(\text{CH}_3\text{COO})_2 \cdot 2\text{H}_2\text{O}$) and 2-propanol were chosen as starting materials to coat ZnO films on glass substrates by sol-gel method. Initially, zinc acetate was dissolved into 2-propanol. Since zinc acetate has low solubility in 2-propanol, diethanolamine (DEA) was added to obtain a transparent solution and to keep the solution stable. The particle size as well as film thickness depend on the molar quantity of diethanolamine (DEA). The molar ratio of zinc acetate and diethanolamine (DEA) was maintained at 1:2. The solution was stirred at a constant temperature 65°C for 1 hour followed by aging for about half an hour to make it cool and stable. Multilayer films were deposited on glass substrates by spin coating method. After each coating, the films were dried at 100°C for 5 minutes. The films thus formed were annealed at different temperatures in oxygen environment. The microstructure and morphology of ZnO films were characterized by X-ray diffractometer (Philips X-Pert MRD) using $\text{CuK}\alpha$ radiation of wavelength 1.5418 \AA at grazing incidence mode and a transmission electron microscope (TEM) operated at 200 kV. Transmittance spectra were recorded by UV-VIS-NIR spectrophotometer in the wavelength range 300-1100 nm. Photoluminescence was measured using a He-Cd laser as an excitation source, operating at 325 nm with an output power of 50 mW and TRIAX 320 monochromator fitted with a cooled Hamamatsu R928 photomultiplier detector.

4. Results and Discussion

Figure 1. TEM images of a grown ZnO film annealed at 450°C . The figure in the inset shows a magnified micrograph.



Typical TEM micrograph of nanocrystalline ZnO film annealed at 450°C is depicted in Figure 1. The micrograph shows particles with narrow size distribution varying within the range 30-35 nm. The

space homogeneity is almost same all over the sample. The porosity level is approximately 15-20% (from the TEM image). Figure 2 shows the intensity– 2θ XRD patterns of the ZnO nanocrystalline films prepared by sol-gel technique. It was found that the film exhibits polycrystalline structure. As indexed in the figure, all diffraction peaks match with the wurtzite structural ZnO. Estimated values of crystallite sizes from XRD pattern are reported in Table 1.

Figure 2. XRD pattern of ZnO films for (a) as deposited, (b) annealed at 250 °C and (c) annealed at 450 °C.

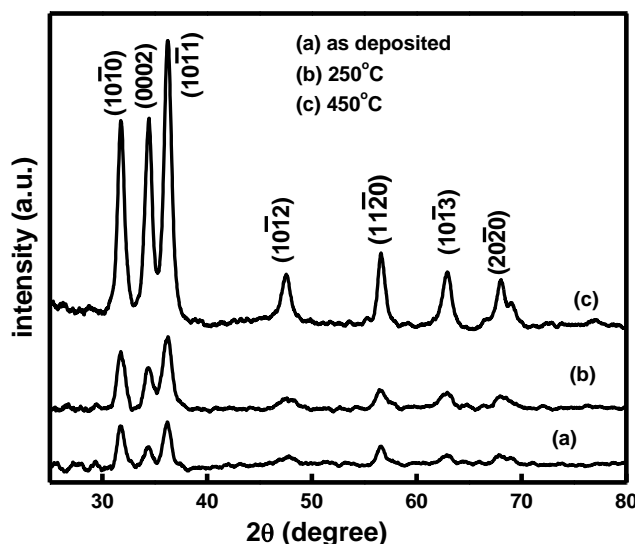


Table 1. Crystallite size of ZnO thin films estimated from the XRD pattern

Description of the Sample	Crystallite Size (nm)
As-prepared	28
Annealed at 250°C	33
Annealed at 450°C	37

The transmittance spectra of grown films in the wavelength range 300nm to 1100nm are shown in Figure 3. They provide useful information about the optical band gap of the semiconductors. The spectra clearly exhibit a shift in band edge due to the variation of substrate temperature, with a transparency of 75 % in the visible range above 400 nm. Sharp ultraviolet absorption edges at approximately $\lambda=380$ nm are observed with the absorption edge being shifted to shorter wavelength at higher anneal temperatures. The absorption coefficient ' α ' can be calculated from the relation: $T = A \exp(-\alpha/d)$, where T is the transmittance of the thin film, A is a constant, and d is the film thickness. The constant A is approximately unity, as the reflectivity is negligible and insignificant near the absorption edge. The optical band gap of the films is determined by applying the Tauc model (Tauc, 1974), and the David and Mott model (David et al., 1970) in the high absorbance region: $\alpha hv = D(hv - E_g)^n$, where hv is the photon energy, E_g is the optical band gap, and D is a constant. For $n=1/2$ the transition data provide the best linear curve in the band-edge region, implying the transition is direct in nature. The band gap of the films has been calculated using Tauc's plot by plotting $(\alpha hv)^2$ versus hv and by extrapolating the linear portion of the absorption edge to find the intercept with energy axis. As the anneal temperature is increased, the optical band gap is found to be red shifted from 3.27 to 3.22 eV.

Figure 3. Transmittance spectra for ZnO films samples (a) as deposited, annealed at (b) 250°C and (c) 450 °C.

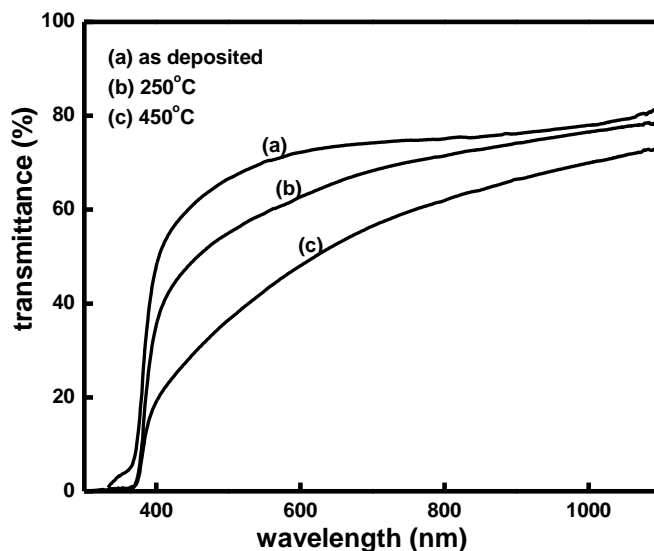
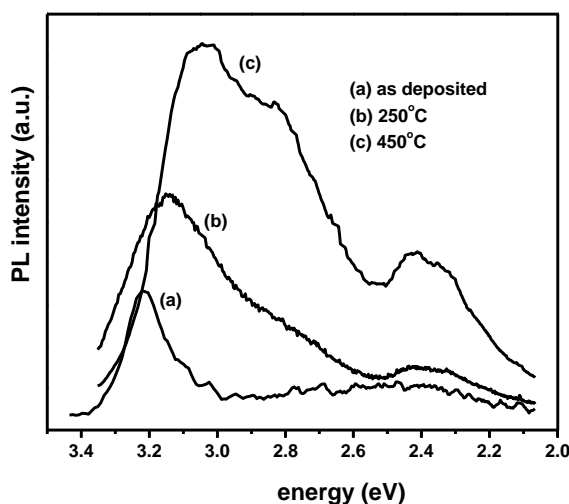


Figure 4 shows the PL spectra for the as deposited ZnO films and the films annealed at 250 °C and 450°C temperatures. Obviously, all the spectra exhibit a relatively sharp and strong ultraviolet (UV) free exciton (FX) emission (Fonoberov et al., 2004) and an emission in the visible range. For the as-grown film, UV emission centers at 383 nm (3.23 eV), the origin of which may be caused by the recombination of surface-bound acceptor exciton complexes. Due to the larger binding energy of the acceptor in ZnO, the band-to-impurity transition is attributed to conduction-band-to-acceptor transition in which free electrons in the conduction band recombine with acceptors.

Figure 4. PL spectra at room temperature for ZnO films (a) as deposited, annealed at (b) 250°C and (c) 450 °C.



After annealing at 250°C and 450°C, the intensity of the emission in the UV range obviously increases and the peak center undergoes a redshift, which shifts to a longer wavelength of 396 nm (3.13 eV) and 403 nm (3.07 eV) respectively. It can be seen that the peak shifted to lower energies with increasing temperature due to the shrinkage of the band gap energy with increasing temperature (Kim et al., 2004). As temperature increases, the bound excitonic feature gets weakened and finally disappears due to the thermal ionization of the BE (Reynolds et al., 1997). All samples showed another characteristic peak at around 512 nm (2.42 eV), which corresponds to the blue-green emission. These emissions were found to be extremely broad and this broadening may be due to phonon assisted transition (Studenikin et al., 1998). Intensity of PL spectra was found to increase with the increases of

annealing temperatures. The center responsible for the blue-green emission in ZnO has not been completely understood. It has been suggested that this peak is associated with oxygen vacancies, and porosity of the films (Xu et al., 2003).

6. Conclusions

We have grown nanocrystalline ZnO films with particles of size 25-30 nm on glass substrates by sol-gel technique. The grazing angle XRD revealed the formation of wurtzite structure ZnO. Our PL measurement shows that the defect energy state is negligible in comparison with band-to-band transition. Overall study shows that sol-gel is one of the simplest techniques to synthesize the high quality nano crystalline ZnO film for the application of optoelectronic device in the ultra violet region.

Acknowledgement

I am grateful to Prof. S. K. Ray (Former professor of IIT Kharagpur, Department of Physics and Meteorology) for giving me the opportunity to provide all the Laboratory facilities.

References

- Liang, W. Y., & Yoffe, A. D. (1968). Transmission Spectra of ZnO Single Crystals, *Physical Review Letter*, 20, 59-62.
- Kityk, I.V., Ebothe, J., Elchichou, A., Addou, M., Bougrine, A., & Sahraoui, B. (2002). Linear Electro-Optics Effect in ZnO–F Film–Glass Interface, *Physica Status Solidi*, 234, 553-562.
- Yang, T. L., Zhang, D. H., Ma, J., Ma, H. L., & Chen, Y. (1998). Transparent conducting ZnO: Al films deposited on organic substrates deposited by rf magnetron-sputtering, *Thin Solid Films*, 326, 60-62.
- Lu, Y. F., Ni, H. Q., Ni, Z. H., Mai, Z. H., & Ren, Z. M. (2000). The effects of thermal annealing on ZnO thin films grown by pulsed laser deposition, *Journal of Applied Physics*, 88, 498-502.
- Bethke, S., Pan, H., & Wessels, B. W. (1988). Luminescence of heteroepitaxial zinc oxide *Applied Physics Letter*, 52, 138-140.
- Ko, H. J., Yao, T., Chen, Y. F., & Hong, S. K. (2000). Photoluminescence properties of ZnO epilayers grown on CaF₂(111) by plasma assisted molecular beam epitaxy, *Applied Physics Letter*, 76, 1905-1907.
- Jeong, S. H., Kim, B. S., & Lee, B. T. (2003). Characterization of the quality of ZnO thin films using reflective second harmonic generation, *Applied Physics Letter*, 82, 2625-2627.
- Shan, F. K., Shin, B. C., Kim, S. C., & Yu, Y. S. (2004). Optical properties of as doped ZnO thin films prepared by pulsed laser deposition technique, *Journal of European Ceramic Society*, 24, 1861-1864.
- Natsume, Y., Sakata, H. (2002). Electrical and optical properties of zinc oxide films post-annealed in H₂ after fabrication by sol–gel process, *Material Chemical Physics*, 78, 170-176.
- Azaroff, L. V. (McGraw–Hill, New York, 1960). *Introduction to Solids*, 371-372.
- Williams, T. M., Hunter, D., Pradhan, A. K., & Kityk, I. V. (2006). Photo induced piezo-optical effect in Er doped ZnO films, *Applied Physics Letter*, 89, 043116-043118.
- Fonoberov, V. A., Alim, K. A., Balandin, A. A., Xiu, F. & Liu, J. (2006). Photoluminescence investigation of the carrier recombination processes in ZnO quantum dots and nanocrystals, *Physical Review B*, 73, 165317-165326.
- Vanheusden, K., Warren, W. L., Seager, C. H., Tallant, D. R., & Voigt, J. A. (1996). Mechanisms behind green photoluminescence in ZnO phosphor powders, *Journal Applied Physics*, 79, 7983-7990.
- Zhang, S. B., Wei, S. H., & Zunger, A. (2001). Intrinsic n-type versus p-type doping asymmetry and the defect physics of ZnO, *Physical Review B*, 63, 075205-075214.
- Tauc, J. (1974) *Amorphous and Liquid Semiconductors*.

David, E. A., & Mott, N. F. (1970). Conduction in non-crystalline systems V. Conductivity, optical absorption and photoconductivity in amorphous semiconductors, *Philosophical Magazine*, 22, 903-922.

Fonoberov, V. A., & Balandin, A. A. (2004). Origin of ultraviolet photoluminescence in ZnO quantum dots: Confined excitons versus surface-bound impurity exciton complexes, *Applied Physics Letter*, 85, 5971-5973.

Kim, K. K., Koguchi, N., Ok, Y. W., Seong, T. Y., & Park, S. J. (2004). Fabrication of ZnO quantum dots embedded in an amorphous oxide layer, *Applied Physics Letter*, 84, 3810-3812.

Reynolds, D. C., Look, D. C., Jogai, B., & Morkoc, H. (1997). Similarities in the bandedge and deep-centre photoluminescence mechanisms of ZnO and GaN, *Solid State Communication*, 101, 643-646.

Studenikin, S. A., Golego N., & Cocivera, M. (1998). Fabrication of green and orange photoluminescent, undoped ZnO films using spray pyrolysis, *Journal of Applied Physics*, 84, 2287-2294

Xu, P. S., Sun, Y. M., Shi, C. S., Xu, F. Q., & Pan, H. B. (2003). The electronic structure and spectral properties of ZnO and its defects, *Nuclear Instruments Methods Physical Review B*, 199, 286-290.